THE ROLE OF MRI IN ASSESSMENT OF ACROMIAL MORPHOLOGY IN ASSOCIATION WITH ROTATOR CUFF TEAR

Thesis

Submitted for Partial Fulfillment of Master Degree In Radio-diagnosis

By
Taha Kamal Hussein Abdelmegeed
(M.B.,B.Ch.)

Supervised by

Prof. Dr. Ahmed Fathy Abdelghany

Professor of Radio-diagnosis
Faculty of Medicine - Ain Shams University

Dr. Ahmed Mohamed Osman

Assistant Professor of Radio-diagnosis Faculty of Medicine - Ain shams University

> Faculty of Medicine Ain Shams University 2020

List of Contents

Ti	Title Page		
•	List of Tables	I	
•	List of Figures	II	
•	Introduction	1	
•	Review of Literature		
	- Anatomy of the shoulder joint	3	
	- MRI shoulder technique	23	
	- Normal shoulder MRI anatomy	32	
	- Pathology of RCT	52	
•	Patients and Methods	66	
•	Results	71	
•	Cases Presentation	79	
•	Discussion	93	
•	Summary and Conclusion	98	
•	References	100	
•	Arabic Summary		

List of Tables

Table No.	Title Pa	ge
Table (1):	Comparison between the two studied groups according to demographic data	1
Table (2):	Comparison between the two studied groups according to acromion type 7	3
Table (3):	Relation between acromion type and demographic data in cases group (n=20)	5
Table (4):	Relation between Acromion type and demographic data in the control group	6
Table (5):	Distribution of the studied cases according to the type of injury	7
Table (6):	Relation between acromion type and type of injury in cases group	8

List of Figures

Figure No.	Title	Page
Fig. (1):	Osteology of bones forming shoulder joint	
Fig. (2):	Glenoid labrum	8
Fig. (3):	The glenohumeral joint capsule lateral view, humerus removed	
Fig. (4):	Ligaments related to the glenohumeral ligament	
Fig. (5):	Bursae related to the shoulder joint .	13
Fig. (6):	(a-b); Coracoacromial arch; type acromion. T1 sagittal oblique image of the shoulder	e
Fig. (7):	Anatomy of deltoid muscle	16
Fig. (8):	Graphic image of a lateral view of the rotator cuff muscles	
Fig. (9):	Graphic image of a posterior view of the supraspinatus muscle	
Fig. (10):	Infraspinatus muscle	19
Fig. (11):	Teres minor muscle	20
Fig. (12):	The subscabularis muscle	21
Fig. (13):	The long head of biceps	22
Fig. (14):	T2 WIS axial planner image showing planning of oblique coronal images	_
Fig. (15):	T2 WIS axial planner image showing planning of oblique sagittal images	_
Fig. (16):	Coronal T1WI SE pulse sequence	27
Fig. (17):	Coronal PD FSE pulse sequence	28

Figure No.	Title	Page
Fig. (18):	Axial GE pulse sequence	29
Fig. (19):	Coronal T2 FSE fat suppression pulse sequence	
Fig. (20):	(a-b): Axial MR anatomy superior images	
Fig. (21):	(a-b) Coronal oblique conventional MRI anatomy	
Fig. (22):	(a-c): Sagittal conventional MR anatomy (mid-sagittal, lateral and medial images)	1
Fig. (23):	Mathematical determination o acromial morphology	
Fig. (24):	(A.B.C) Methods of measuring acromio-humeral distance (AHD)	_
Fig. (25):	Normal acromiohumeral intervals T1 coronal oblique image of the shoulder	2
Fig. (26):	Subacromial/subdeltoid bursal fat low-lying acromion. A, T1 corona oblique image of the shoulder	1
Fig. (27):	Acromion orientation. A: Corona oblique T1-weighted image shows low lying acromion	3
Fig. (28):	Anterior-sloping acromion. To sagittal oblique image of the shoulder	e

Figure No.	Title Page	3
Fig. (29):	Acromial slope: inferolateral tilt. T1 coronal oblique image of the shoulder	
Fig. (30):	Acromial orientation. FSE T2 oblique coronal images showing the relationship of the acromion to the distal clavicle in three different shoulders	
Fig. (31):	Types of acromial shape 49	
Fig. (32):	Os acromiale. T2* axial image of the shoulder	
Fig. (33):	Coronal graphic shows a partial undersurface tear of the articular surface of the supraspinatus tendon involving the critical zone	
Fig. (34):	Coronal graphic shows a bursal surface partial tear with reactive bursal changes	
Fig. (35):	Coronal graphic shows an interstitial delaminating partial tear 54	
Fig. (36):	Coronal graphic shows a full thickness tear through the mid substance of the supraspinatus tendon	
Fig. (37):	Focal full-thickness supraspinatus tendon tears	
Fig. (38):	Partial-thickness tendon tears 57	

Figure No.	Title	Page
Fig. (39):	Thinning of the rotator cuff. Coronal oblique fat-saturated T2-weighted MR image shows thinning of the supraspinatus tendon (arrow)	l ;
Fig. (40):	Medial tendon retraction	60
Fig. (41):	Factors affecting the medial extent of a tendon tear	
Fig. (42):	Sagittal extent of rotator cuff tears as described by Thomazeau et al	
Fig. (43):	Drawing illustrates use of the sagittal plane (dashed line) relative to the coracoid base and acromial spine for estimating volume loss in the supraspinatus muscle	
Fig. (44):	Sagittal fat-saturated T2-weighted MR image shows a normal occupation ratio, representing the ratio between the cross-sectional area (green) of the belly of the supraspinatus muscle (SST) and that of the scapular fossa (orange)	l : : :
Fig. (45):	Abnormal occupation ratio. Sagittal fat-saturated T2- weighted MR image shows volume loss in the supraspinatus muscle (SST), whose cross-sectional area (green) is now much smaller than that of the scapular fossa (orange)	
Fig. (46):	Tangent sign	65

Figure No.	Title	Page
Fig. (47):	Comparison between the two studie groups according to acromion type	
Fig. (48):	Relation between acromion type an type of injury in cases group	

ABSTRACT

Background: The pathogenesis of rotator cuff tear (RCT) remains controversial. The acromion portion of the scapula and its morphology may be attributable for a variety of shoulder disorders such as RCT.

Patients and Methods: This was a retrospective study that included 40 patients divided into two groups; a group with RCT included 20 patients and a control group with no RCT included the other 20 patients. 19 were males and 21 females, their age 20-69 years old with a mean age of 45. Cases were selected from the PACS system of the Radiology department of Ain Shams University Hospital. Statistical data analysis was done using IBM SPSS software package version 20.0. (Armonk, NY: IBM Corp)

Results: The study revealed that Type II acromion was encountered in most of the male patients (42.1%) and type III acromion was encountered in most of the female patients (42.9%) while type IV acromion was less frequently seen among males and females (5% & 0%) respectively. It also revealed that Type III is mostly encountered in RCT (50%); 58% of full-thickness tear and 37% of partial thickness tear. while type I is less frequently associated with a partial tear or full-thickness tear (8%) for each.

Acromion type III was the commonest type of acromion found between the patients of the case group with a significant statistical difference found between the case and control groups

(P value: 0.006). However, type I acromion was the commonest acromion type found between the control group with also a significant statistical difference (P value: 0.011).

Conclusion: Type III acromion may be a risk factor leading to rotator cuff tear. This may help guide therapy in patients with shoulder pain and findings suggesting type III acromion shape

Keywords: acromion shapes, magnetic resonance imaging, rotator cuff tear

INTRODUCTION

The acromion is a posterior shoulder landmark, formed as a postero-lateral extension of the scapular spine, superior to the glenoid. It articulates with the clavicle and is the origin of the deltoid and trapezius muscles, Variation in the shape of the acromion can endorse variety of pathologies such as impingement syndrome and rotator cuff tear (RCT) (Mansur et al., 2013).

The acromial shape can be classified into four types: type I (flat), type II (curved), type III (hooked) and type IV (convex) (Guishan et al., 2013).

Rotator cuff disorder is one of the most common disorders of the shoulder. It is a common cause of chronic shoulder pain in adults. The specific etiology of a RCT has not been fully elucidated, but it has been considered to result from a combination of intrinsic and extrinsic factors. Intrinsic factors include degenerative changes, hypovascularity, microstructural fiber and collagen Recognized abnormalities. extrinsic factors include subacromial impingement, tensile overload and repetitive use (Yamamoto et al., 2017).

The pathogenesis of RCT seems to be related to the morphology of the acromion which is usually assessed through the five commonly used parameters on standard plain radiographs including the acromial type, acromial

slope, acromial tilt, lateral acromial angle and acromial index (Alobaidy et al., 2015).

However, with only a plain radiograph of the acromion in the supraspinatus outlet view, it is difficult to image the acromion and distinguish the hooked from the non-hooked acromion with anterior spurs (*Jacinth et al.*, 2018).

The magnetic resonance imaging (MRI) makes it possible to depict the shape of acromion in its longitudinal axis with better evaluation of the acromial morphological factors including the acromial shape, acromial thickness, acromio- humeral distance, and lateral acromial angle and acromial index. These factors are suggested to influence the status of the rotator cuff (Gumina et al., 2017).

CHAPTER (1): ANATOMY OF THE SHOULDER JOINT

The shoulder joint is a ball-and-socket synovial joint in which an elegant freedom of movement is allowed at some expense to its strength and stability.

The bones entering in its formation are the hemispherical head of the humerus (ball) linking to the shallow glenoid cavity of the scapula (socket). Some protection of the joint against displacement is afforded by its ligaments and by the tendons and muscles that surround it. The ligamentous protection supplied by the muscles and tendons effectively limits the degree of movement allowed by the joint. Additional protection superiorly supplied by the arch formed by the coracoid process, acromion, and coracoacromial ligament (*Taylor et al.*, 2016).

The clavicle connects the axial and appendicular skeletons of the upper extremity. Its sternal end is expanded and fits into the notch on the manubrium at the sternoclavicular joint. The lateral one-third is flat, and its lateral end is expanded as it curves back to meet the scapula at the acromioclavicular joint (*Piper et al., 2018*).

The scapula consists of the scapular body, the scapular spine, the scapular neck, the acromion, the glenoid fossa, and the coracoid process. It has costal (anterior) and

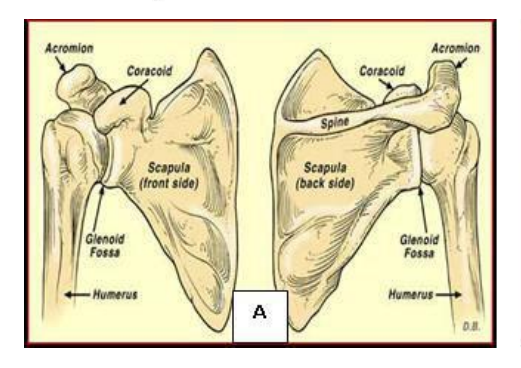
posterior surfaces with its anterior surface in contact with the thoracic cage (the scapula-thoracic interface). From the upper part of the posterior surface, the spine of the scapula projects laterally, terminating into the acromion, which forms the lateral most tip of the shoulder (*Fig. 1*) (*Piper et al., 2018*).

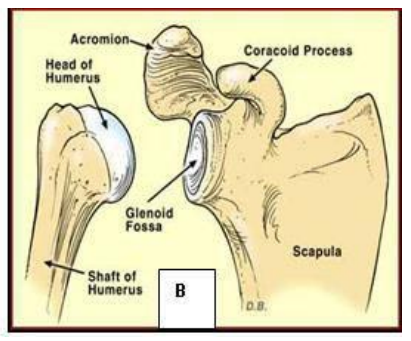
The lateral angle of the scapula is thick and strong, with an expanded large, shallow glenoid fossa,. Just medial to the glenoid fossa is the coracoid process as it projects upwards from the neck of the scapula. The coracoid process serves as an attachment site for several important ligaments and muscles (*Fig 1*) (*Bleichert et al.*, 2017).

The proximal humerus consists of the head, anatomic neck, and the greater and lesser tuberosities. The intertubercular or bicipital groove is located between the greater and lesser tuberosities along the anterior surface of the humerus (Kadi et al., 2017).

The head of the humerus is approximately one third of a sphere and it is about four times larger than the socket on the scapula. In anatomic position, it faces superiorly, medially, and posteriorly with the lesser tuberosity in front and the greater tuberosity pointing laterally (*Fig. 1*) (*Patel et al.*, 2018).

.Review of Literature





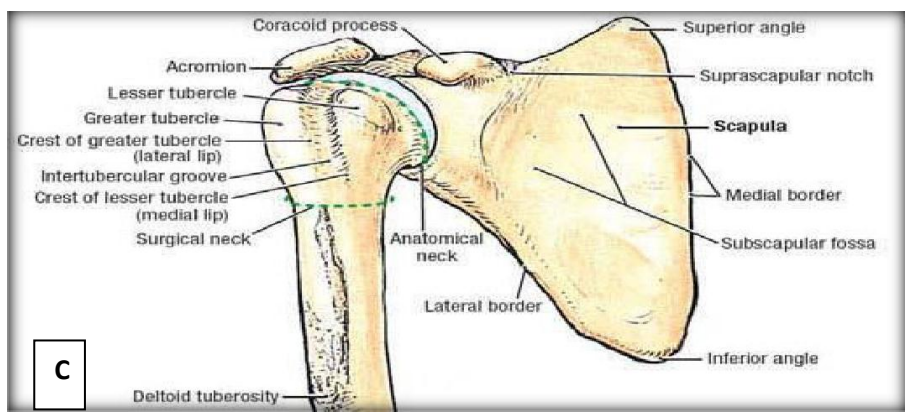


Fig. (1): (a-c) Anatomy of bones forming shoulder joint (Piper et al., 2018) and (Patel et al., 2018).

Joints of the shoulder girdle

I- Glenohumoral joint

The glenohumeral joint is a multiaxial spheroid joint. The great freedom of movement of the glenohumeral joint is inevitably accompanied by a considerable loss of stability. To compensate for this, the joint is reinforced by the tendons of the rotator cuff. In addition, the joint capsule has a rather complex structure consisting of the labrum and the glenohumeral ligaments, known as the labral capsular complex that further aids stability (*Mostafa et al., 2012*).

As the convexity of the humerus is much larger than the glenoid cavity, only a minor part of it can be in contact with the cavity in any given position of the joint and the remainder of its articular surface is in contact with the inner aspect of the capsule. Both articular surfaces are covered with a layer of hyaline cartilage that on the head of the humerus is thickest at its center and thinner peripherally, with the reverse is the case in the glenoid cavity. However, in most positions of the joint, the curvature of the adjacent parts of the surfaces are not precisely the same i.e. they are not congruent and the joint is loosely packed. Full congruence and close packed position is reached when the humerus is abducted and laterally rotated. The glenoid cavity is deepened somewhat by a fibrocatilagenous rim attached to its margins, the glenoid labrum (Adams et al., *2016*).

The Glenoid labrum

It is the fibrous attachment of the glenohumeral ligaments and capsule to the glenoid rim around the margin of the glenoid cavity. It is triangular in section, the base being fixed to the circumference of the cavity, while the free edge is thin and sharp. Measuring about 6mm in width and 3mm in height, the labrum is somewhat shallower on the sides of the cavity. It deepens the articular cavity and protects the edges of the bone. It increases the surface of articulation with humeral head and serves as anchoring mechanism distributor of stress forces for the capsular